Quantum Electronics **48** (7) 596–602 (2018)

https://doi.org/10.1070/QEL16679

Influence of molecular oxygen addition on gain and generation characteristics of a cryogenic slab RF-discharge-pumped overtone CO laser

A.A. Ionin, A.Yu. Kozlov, I.V. Kochetov, A.K. Kurnosov, A.P. Napartovich, O.A. Rulev, D.V. Sinitsyn

Abstract. **The influence of molecular oxygen addition to an active medium of a cryogenic slab RF-discharge-pumped overtone CO laser operating without active medium circulation on the threshold generation conditions and spectral and energy characteristics of laser radiation is calculated. Results of the modelling well agree with experimental data obtained at the initial period of laser operation and substantially differ from data obtained after reaching a stationary operation regime. The model sufficiently well describes characteristics of a single-pulse electron-beam controlled CO laser operated on gas mixtures comprising oxygen. In this model, the generation pulse profiles of a cryogenic slab CO laser operated on the fundamental band transitions of the CO molecule under pulsed-periodic RF pumping well agree with experimental data. The agreement is also observed for the parts of the RF-discharge power spent on exciting vibrational and electronic states of molecules. Reasons for distinctions between some other calculated and experimental data are analysed.**

Keywords: *slab CO laser, overtone transitions, model calculation, oxygen addition, transverse RF discharge.*

1. Introduction

Among all types of gas lasers, planar (slab) constructions pumped by a radio-frequency (RF) discharge are the most compact and possess a high specific radiation power. Heat from the active medium of such lasers is released due to thermal diffusion through electrode surfaces. The electrodes themselves can be cooled by using various cooling agents down to cryogenic temperatures. CO lasers are especially sensitive to the temperature of the active medium [1–3]. Their efficiency and the width of the emission spectral band noticeably grow under deep cooling of the active medium, and efficient generation on overtone transitions of CO molecule was only obtained at cryogenic temperatures [4]. Until quite recently, cw and pulse-periodic CO lasers with cryogenic cooling operated only if the active medium circulated through the discharge volume (see, for example, [5–7]). Under deep cooling, idue to the plasma-chemical reactions which inevitably occur in a gas discharge plasma with participation of CO molecules, some products condensate on cool internal elements of the construction, thus escaping participation in reverse reactions that are efficient at higher temperatures. As a result, the active medium degrades, and further operation of the CO laser with cryogenic cooling requires gas mixture recirculation during the emission process. This, in turn, increases complexity and size of such lasers. This is why the number of works devoted to cryogenic planar (slab) cw and pulse-periodic CO lasers without active medium recirculation is rather limited [8–10].

Recently, in the Gas Lasers Lab of the P.N. Lebedev Physical institute, a slab RF-discharge-pumped CO laser with cryogenic cooling of electrodes was developed, which can operate for a sufficiently long time in a quasi-sealed-off regime [11–14]. In this case, the average power of radiation on overtone transitions of the CO molecule reached 2 W in the wavelength range 3.0-3.5 μm [14]. Such results were obtained by using as an active medium the gas mixtures with an anomalously large initial content of oxygen for CO lasers, up to 50% relative to the CO molecule concentration.

In experiments [11–14], it was found that at high initial concentrations of O_2 ($[O_2] \sim 0.5[CO]$), lasing started with a delay of several minutes after the pulse-periodic RF-discharge switched on. After the average radiation power reached a stationary level, the service life of the laser to a noticeable degradation of the gas mixture and emission termination (the whole operation cycle) was above 10^6 pulses (at a pulse repetition rate of 300–400 Hz, the operation lasted for ~1 hour). While using an oxygen-free CO–He mixture, emission started immediately after the discharge was switched on; however, it quickly (in 1–2 min) ceased. In addition, in the whole operation cycle of the laser without mixture recirculation, certain peculiarities were observed, which have not been explained, namely: at the O_2 initial concentration in the range (0.1–0.3)[CO], lasing started after the RF-discharge was switched on, the starting level of the output power being greater at lower O_2-concentration. The stationary level of the laser power in this case corresponded to the initial output power of a laser with oxygen-free mixture. Approximately in the middle of the whole operation cycle, in all regimes the output power relatively rapidly increased (by ~15% per 1–2 min).

Theoretical analysis of the effects observed determines the aim and main contents of the present work. We present results of theoretical calculations of the parameters and characteristics of a sealed-off slab CO laser with cryogenic cooling of electrodes pumped by a pulse-periodic RF-discharge and

A.A. Ionin, A.Yu. Kozlov, O.A. Rulev, D.V. Sinitsyn P.N. Lebedev Physical Institute, Russian Academy of Sciences, Leninsky prosp. 53, 119991 Moscow, Russia; e-mail: aion@sci.lebedev.ru;
I.V. Kochetov, A.K. Kurnosov, A.P. Napartovich P.N. Lebedev Physical Institute, Russian Academy of Sciences, Leninsky prosp. 53, 119991 Moscow, Russia; State Research Center of Russian Federation 'Troitsk Institute for Innovation and Fusion Research', ul. Pushkovykh, vladenie 12, Troitsk, 142190 Moscow, Russia

Received 20 March 2018; revision received 11 May 2018
Kvantovaya Elektronika **48** (7) 596–602 (2018)
Translated by N.A. Raspopov

operated on $CO-O_2-He$ gas mixtures [14]. We also discuss the influence of the active medium content variations resulting from plasma-chemical processes on laser characteristics.

2. Theoretical model

CO laser characteristics were calculated in the frameworks of the spatially homogeneous model, in which the near-electrode layers are neglected in considering RF-discharge characteristics. The value of a reduced electric field in plasma was determined by the equality of rates of electron production/loss processes; in the conditions of the experiment, it was ~20 Td. The electron concentration in the RF-discharge was calculated for a positive column in a dc-discharge assuming that the calculated power deposited into the dc-discharge is equal to the measured power of the RF-discharge. The applicability of this approach was substantiated in [15]. A comparison of the reduced electric field and electron concentration, calculated in this way, with the results of RF-discharge modelling in the frameworks of one-dimension model [16] shows a reasonable agreement between those.

The gains and generation characteristics of a CO laser operated on the fundamental band transitions ($v + 1 \to v$; v is the vibration level number) or on transitions of the first vibration overtone ($v + 2 \to v$) were calculated by solving vibrational kinetic equations for the active medium comprising a $CO-O_2-He$ gas mixture at a total pressure $p = 22$ Torr and initial temperature $T_0 \sim 110$ K, in which oxygen is a small additive. These equations were solved jointly with the Boltzmann equation for the electron energy distribution function (EEDF), which allowed one to account adequately for the energy exchange between electrons and molecule vibrations. The pressure of the active medium was assumed constant, which is justified by the presence of a substantial buffer volume (~15 L) that multiply exceeds the volume of the RF-discharge (~20 cm^3). Diffusion of vibrationally excited molecules to electrodes and the following heterogeneous relaxation were taken into account in the τ-approximation [17]. Under these assumptions, the system of equations describing evolution of vibration level populations n_v of CO molecules up to the level $v = 50$ and molecules O_2 to level $v = 20$ in a central domain of the RF-discharge has the form:

$$\frac{dn_v}{dt} = R^v_{eV} + R^v_{VV} + R^v_{sp} + R^v_{ind} - \frac{n_v}{\tau_d} - \frac{n_v}{T}\frac{dT}{dt}, \qquad (1)$$

where R^v_{eV}, R^v_{VV}, R^v_{VT}, R^v_{sp}, and R^v_{ind} are the rates of variation of a vibrational level with number v population by electron impact, by VV-exchange and VT-relaxation processes, in spontaneous and induced emission, respectively; τ_d is the diffusion time; and T is the gas temparature. These terms of the kinetic equations were calculated in the frameworks of the theoretical model for an active medium of the electric-dicharge CO laser described in [4, 18] and generalised in [19] to the case of oxygen-containing $CO-O_2-He$ mixtures. Note that the model used well describes the gain dynamics on various transitions of a single-pulse electron-beam controlled CO laser with an oxygen-containing active medium [19].

The diffusion time τ_d was calculated taking into account the geometry of the active volume in which the width of the interelectrode gap L is far less than the length and height [17, 20]:

$$\tau_d = \frac{\Lambda^2}{D} + \frac{2-\varepsilon}{\varepsilon}\frac{L}{\bar{u}}, \qquad (2)$$

where $\Lambda = L/\pi$ is the characteristic diffusion length; D is the diffusion factor for CO molecules in He [21]; ε is the coefficient of vibrationally excited molecule accommodation on the wall; and $\bar{u}$ is the average velocity of molecule thermal motion. The second summand in (2) takes into account heterogeneous relaxation of vibrationally excited molecules in studied operation regimes of the CO laser. The value of CO molecule accommodation on the wall, which depends on the electrode material and other factors, is unknown. In the calculations, a weak sensitivity was revealed of the results of the modelling of the laser gain and generation characteristics to the parameter ε varied in the range 0.05–0.5. Note that the contribution of the processes mentioned into kinetic equations (1) increases with decreasing gas pressure.

Temperature T of the active medium was calculated taking into account its direct heating in the discharge, the heating due to dissipation of the vibration energy in VV-exchange and VT-relaxation processes, and cooling due to heat removal through cooled electrodes, which was taken into account in the τ-approximation:

$$\frac{dT}{dt} = \frac{W}{kNC_p} + \frac{W^*}{kNC_p} - \frac{T - T_0}{\tau}, \qquad (3)$$

where W is the specific power of direct heating; W^* is the power of dissipation losses; k is the Boltzmann factor; N is the particle concentration; C_p is the mixture specific heat at a constant pressure; T_0 is the wall temperature; $\tau = kNC_pL^2/(\lambda\pi^2)$; and λ is the coefficient of thermal conductivity for the mixture, which was found from the values of coefficients of thermal conductivity for separate gases [22] by the procedure described in [23].

A calculated part of the pump power loaded to vibrations of the CO molecules depended on the degree of their vibrational excitation. For example, at the RF-discharge pulsed power $P_{RF} = 350$ W, $F = 400$ Hz, and the duty factor $s = 20\%$ (F is the RF-discharge pulse repetition rate, s is the ratio of the pulse duration to the pulse-repetition interval), this part in the $CO:He = 1:10$ and $CO:O_2:He = 1:0.1:10$ mixtures was on the average ~60%. The part of a discharge power expended for excitation of CO molecule electronically excited states was ~40%; in these conditions, approximately half of this value was spent on direct heating of the mixture.

The intensity of laser radiation I_{vj} on the vibrational–rotational transition $v + m, j - 1 \to v, j$ ($m = 1$ is the fundamental vibrational band and $m = 2$ is the overtone band of the CO molecule) near the cavity axis coinciding with the principal axis of the active interelectrode volume was calculated under simplest assumptions by using the photon balance equation in the cavity:

$$\frac{dI_{vj}}{dt} = c(g_{vj} - G_{th})I_{vj} + \frac{Z\Omega}{4\pi}n_{v+m}A_{v+m}, \qquad (4)$$

where c is the speed of light; Z is the cavity length; Ω is the angular aperture of outcoupling mirror; g_{vj} and G_{th} are the gain on the considered vibrational–rotational transition and its threshold value, respectively; and n_{v+m} and A_{v+m} are the population of upper vibrational level and Einstein coefficient for the considered vibrational transition.

Characteristics of the cryogenic slab CO laser [14, 24] were calculated, in which the active medium was excited by a pulsed-periodic capacitive transverse RF-discharge with a carrier frequency of 60 MHz. The interelectrode gap was

3 mm, the electrode width was 16 mm and the length was 400 mm.

3. Calculation results and discussion

3.1. Dynamics of the active medium temperature

Calculated dynamics of the gas temperature at the principal axis of the active interelectrode volume at P_{RF} = 350 W, F = 400 Hz, and s = 20% is presented in Fig. 1 both in the case of laser emission and when the latter is absent. Calculations performed for $CO-O_2-He$ gas mixtures with various contents of O_2 show that in these excitation conditions a stationary temperature regime is already attained to the third pump pulse, and the temperature difference with and without laser emission is not above 10 K.

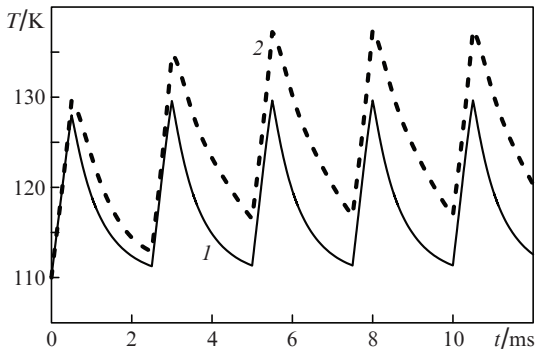

Figure 1. Dynamics of the active medium temperature calculated in the case of (*1*) generation and (*2*) without it at P_{RF} = 350 W, F = 400 Hz, s = 20%; the mixture is $CO:O_2:He = 1:0.3:10$, p = 22 Torr.

3.2. Influence of molecular oxygen addition to the active medium on a small-signal gain and threshold conditions for laser emission of the overtone CO laser

Calculated dynamics of a small-signal gain (SSG) in a central part of the active medium near the cavity axis gives information whether laser emission is possible or not under varied parameters of the cavity or active medium. The study of the influence of molecular oxygen addition to the active medium of an RF-discharge-pumped CO laser on the SSG dynamics is of high interest. Calculations of SSG dynamics on transitions in the overtone band show that addition of molecular oxygen to the initial mixture substantially affects the value of SSG, output power, and laser emission spectrum (in contrast to the fundamental band, where the value of SSG is much greater and the influence of molecular oxygen addition to the $CO:He = 1:10$ mixture was negligible). For this reason, the most of calculations were performed for the overtone band of the CO molecule. Results of SSG calculations are presented in Fig. 2 for transitions in six overtone vibrational bands of the CO molecule in $CO-O_2-He$ mixtures with various molecular oxygen contents X. In these figures, dependences (*1–6*) correspond to the vibrational–rotational transitions $v + 2 \rightarrow v$ P(J) (J is the rotational quantum number for the lower vibrational level of the transition) 18 → 16 P(12), 19 → 17 P(12), 20 → 18 P(12), 21 → 19 P(12), 23 → 21 P(12), and 31 → 29 P(12) possessing the emission wavelengths in the spectral range from 2.95–3.63 μm. In the figures, time is counted from the moment of first discharge pulse switching on [to the fifth pulse, the start of which corresponds to 10 ms, a steady temperature regime of the active medium is established (see Fig. 1)].

In the $CO:He = 1:10$ mixture (X = 0), the calculated SSG dynamics on transitions between high vibrational levels points to possible wide-band emission in the overtone band.

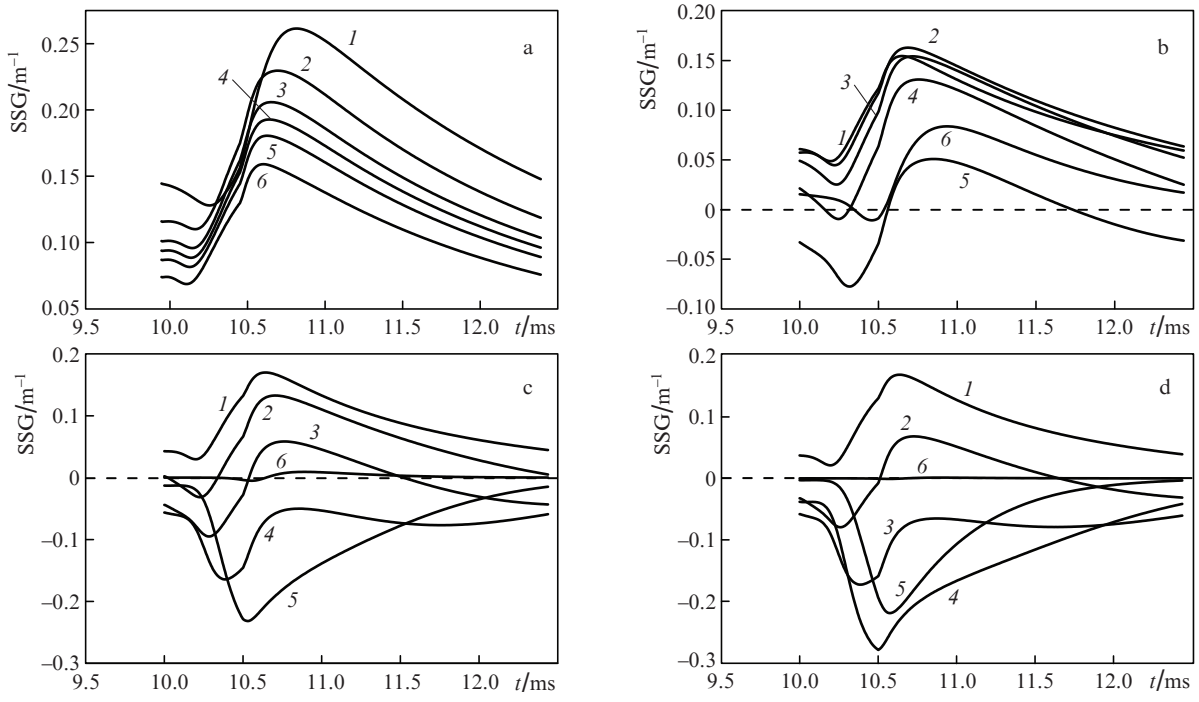

Figure 2. SSG dynamics on transitions of the first vibrational overtone in the active medium of a cryogenic RF-pumped CO laser with various oxygen contents at P_{RF} = 350 W, F = 400 Hz, s = 20%, $CO:O_2:He = 1:X:10$, X = (a) 0, (b) 0.1, (c) 0.3, (d) 0.5; the transitions are $v + 2 \rightarrow v$ P(12), v = 16 (*1*), 17 (*2*), 18 (*3*), 19 (*4*), 21 (*5*), and 29 (*6*).

In the $CO:O_2:He = 1:0.1:10$ mixture, the gain on all transitions substantially falls. In the $CO:O_2:He = 1:0.3:10$ mixture, the gain on the transition $20 \rightarrow 18$ P(12) [curve (*3*) in Fig. 2c] is not above 0.05 m^{-1}, and on transitions between higher levels anly absorption should be observed instead of amplification. In the $CO:O_2:He = 1:0.5:10$ mixture (Fig. 2d), amplification is absent for all transitions with $v > 17$. In view of the fact that the wavelength corresponding to transitions of this band is approximately 3 μm, no shorter-wavelength transitions can appear in the spectrum as well, because at $\lambda < 3$ μm the threshold gain in the cavity used in our experiments rapidly increases at shorter laser emission wavelengths, which is illustrated in Fig. 3. Hence, in the considered experimental conditions, no overtone emission in the mixture $CO:O_2:He = 1:0.5:10$ should be observed.

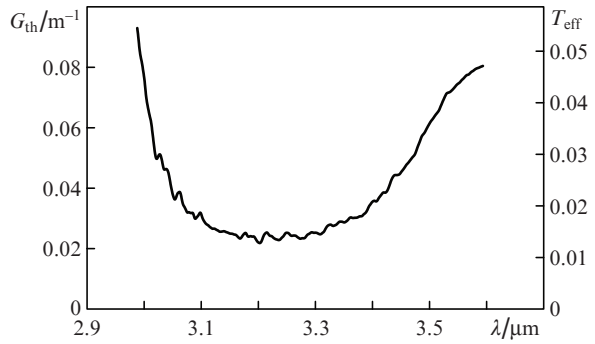

Figure 3. Spectral dependence of effective transparency T_{eff} of the laser cavity used in experiments [14], and threshold gain values G_{th} on overtone transitions of the CO molecule calculated in these conditions.

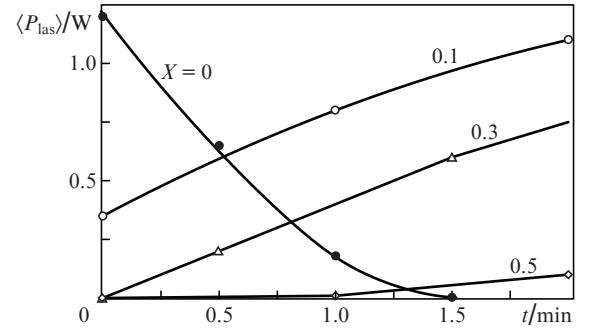

Figure 4. Time dynamics of the average radiation power of the overtone CO laser at various oxygen initial concentrations in the mixture $CO:O_2:He = 1:X:10$ [14, 24].

3.3. Influence of molecular oxygen addition to the active medium on the calculated characteristics of laser emission on overtone band transitions of the CO molecule

3.3.1. Generation power of an overtone CO laser. Calculation results for SSG dynamics on overtone band transitions of the CO molecule with O_2 addition give the idea how these additives affect the dynamics of the average laser power observed in experiments, with the cavity characteristics given in Fig. 3. Time dependences of the average power of the overtone CO laser measured in experiments [14, 24] are shown in Fig. 4 for various initial oxygen concentrations X in the $CO:O_2:He = 1:X:10$ mixture.

These experiments show that if O_2 is not added, generation on overtone transitions ceases in 1–1.5 min (a similar effect was observed in the fundamental band). In this case, the main channel of active medium degradation in an RF-discharge is the process of carbon oxide dissociation followed by freezing of the products of this process (C and CO_2) on cryogenic internal elements of the laser chamber (see, for example, [25–27]).

From these experimental data one can also see that directly after switching on the RF-discharge, the laser power for the $CO:O_2:He = 1:0.3:10$ and $1:0.5:10$ mixtures is close to zero, which is explained by a high initial O_2 concentration in the active medium. Consideration of SSG dynamics in these mixtures (see Figs 2c and 2d) makes one to conclude that with the cavity characteristics from Fig. 3, generation on overtone transitions in the bands from $20 \rightarrow 18$ to $31 \rightarrow 29$ is not possible. Possible generation in the bands $18 \rightarrow 16$ and $19 \rightarrow 17$ should be inefficient due to a negligible excess of gain over the threshold value.

The fact that in using the $CO:O_2:He = 1:0.3:10$ and $1:0.5:10$ gas mixtures, the lasing on the overtone transitions occurs only after a certain time interval after switching on the RF-discharge can be explained by a reduction of molecular oxygen content X in the mixture during this interval down to $X < 0.3$ (at least in the active volume between electrodes). The following radiation power growth and attaining the maximal values points, first of all, to further reduction of a gas-phase O_2 concentration in the active volume and weakening of the contribution of VV′-exchange processes between vibrationally excited CO molecules and O_2 molecules on low vibrational levels into the population kinetics of CO molecules on highly excited vibrational levels. The reduction of O_2 molecule concentration in time, seemingly, is explained by molecular oxygen dissociation in the RF-discharge with production of atomic oxygen and ozone and participation of these products in various homogeneous and heterogeneous chemical reactions. Probably, the latter play a substantial role in real experiments; however, those can hardly be taken into account in the modelling.

By comparing a current value of the laser power with its initial value at small addition of O_2 one can judge the absolute value of molecular oxygen concentration reached at this moment in the active volume between electrodes. For example, from dependences in Fig. 4 one may conclude that in the case of the mixture with the initial oxygen concentration $X = 0.3$, in a time moment of ~1 min after switching on the RF-discharge, the O_2 concentration in the active volume should fall to $X \sim 0.1$, because the average laser power at this moment approximately equals the power of laser operated on the mixture with $X = 0.1$ at the initial moment ($t = 0$).

Thus, the value of the laser power on overtone transitions in the cavity possessing characteristics from Fig. 3 can be used for determining the current O_2 concentration in the active volume of the RF-discharge-pumped CO laser in question.

Calculated and experimentally measured dependences of the average laser generation power $\langle P_{las}\rangle$ on CO molecule overtone transitions are shown in Fig. 5 as functions of the initial molecular oxygen concentration X, obtained with the cavity characteristics from Fig. 3. The calculated dependence is normalised in such a way that the calculation results coincide with results of measuring the average power for the oxygen-free CO–He mixture ($X = 0$). The experimental values in the figure are determined at the initial moment of laser operation, when the initial gas mixture composition in the active volume is not changed yet.

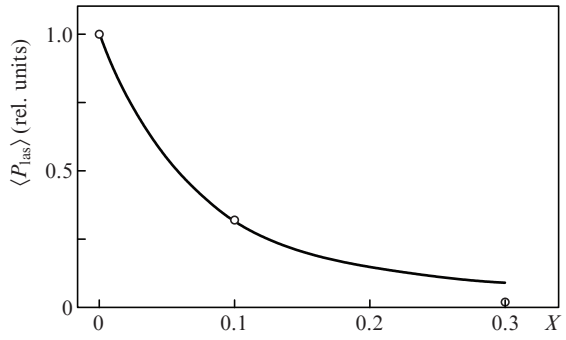

Figure 5. Calculated average generation power on CO molecule overtone transitions as a function of oxygen contents X in the initial $CO:O_2:He = 1:X:10$ mixture at $P_{RF} = 350$ W, $F = 400$ Hz, $s = 20\%$. Points denote experimental data corresponding to the initial conditions from Fig. 4 at $t = 0$.

3.3.2. Generation spectra of the overtone CO laser. Calculation results for the average generation power and the results of modelling the SSG dynamics discussed above reveal a strong dependence of the overtone generation power on the concentration of O_2 in the laser active volume. Spectra of laser radiation on overtone vibrational band transitions of the CO molecule calculated for $X = 0.1$ and 0.3 are shown in Fig. 6 in the same scale.

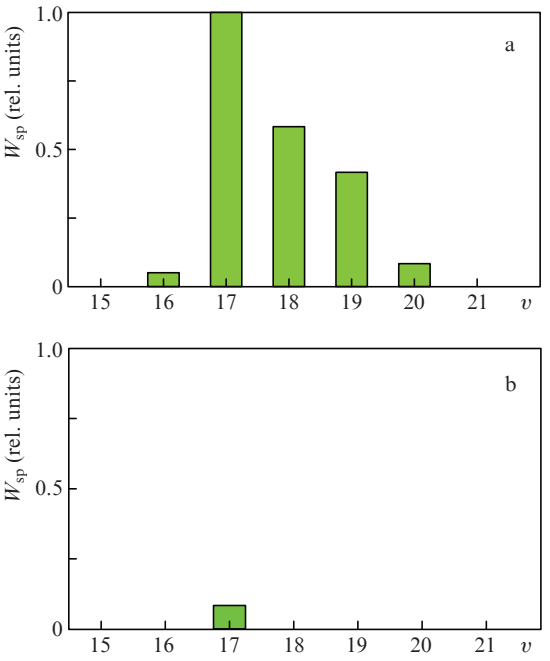

Figure 6. Spectra of laser radiation on transitions $v + 2 \rightarrow v$ of the CO molecule overtone vibrational band using the $CO:O_2:He = 1:X:10$ gas mixtures with $X =$ (a) 0.1 and (b) 0.3. The parameters used in calculations are given in Fig. 5.

The power at each vibrational transition $v + 2 \rightarrow v$ is the result of summing over all its rotational components. The calculated spectra of laser overtone generation (Fig. 6) is yet another illustration of the strong influence of molecular oxygen concentration in the CO laser active volume on the possibility of generation on high vibrational levels at $v \geqslant 19$.

3.4. Generation of the CO laser on fundamental band transitions

To approve adequacy of the theoretical model and approximations used we calculated time profiles of generation pulses of the CO laser investigated in [13], which operated on transitions of the fundamental band ($v + 1 \rightarrow v$) of the CO molecule (Fig. 7).

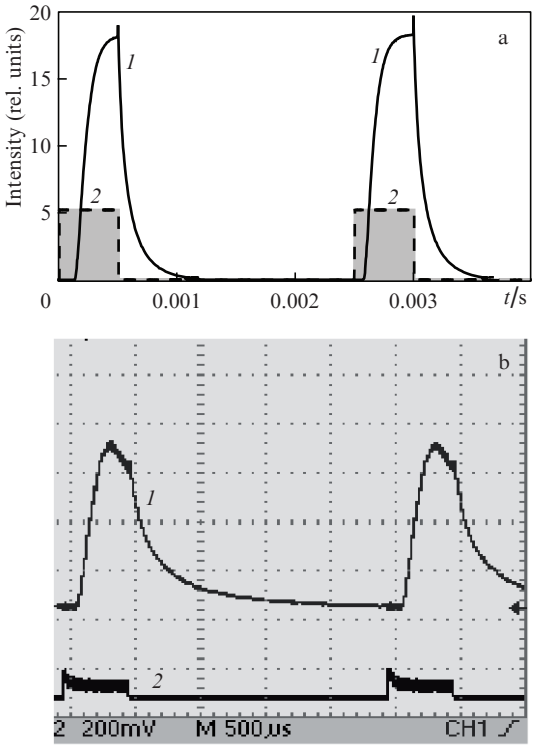

Figure 7. (a) Calculated and (b) experimentally measured in [13] time profiles of (*1*) laser radiation intensity and (*2*) RF-pump power at $P_{RF} = 350$ W, $F = 400$ Hz, $s = 20\%$.

In these calculations, the main characteristic, in addition to common similarity of the laser pulse time profiles, was the laser pulse delay relative to the start of RF-pump pulse. From Fig. 7 one can see that in similar initial conditions, the theoretical and experimental values of this parameter well agree.

In addition, in the conditions of experiments [13, 14, 24], the average radiation power of a laser operated on fundamental band transitions was calculated as a function of the CO content in the mixture, which, according to experiments [24], reduces during the operation cycle. The initial mixture was $CO:He = 1:10$. Then mixtures with a lower CO content were considered. The calculation results are shown in Fig. 8. Dependence (*1*) in the figure is obtained under the assumption that all the pump power spent on pumping electronically excited states additionally contributes to direct heating. As the concentration of the CO molecules reduces, this power increases, and the power used to excite CO molecule vibrations in the discharge falls. Dependence (*2*) is calculated under the assumption that only 50% of the power spent on excitation of electronically excited states contributes to direct heating. Dependence (*1*) is calculated under the assumption that the parts of the pump energy passing to mixture heating and to excitation of CO vibrations do not change. It can only be justified if variations of the CO molecule concentration are negligible.

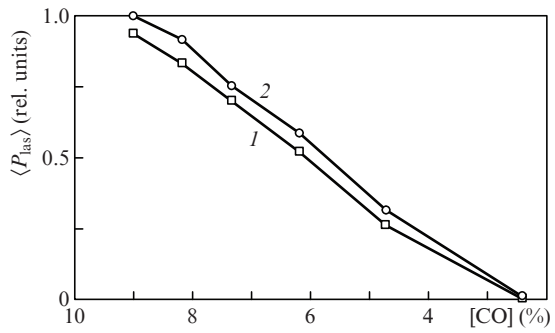

Figure 8. Calculated average power of laser generation on transitions of the fundamental band as a function of CO molecule concentration in the initial mixture at P_{RF} = 350 W, F = 400 Hz, s = 20%.

A substantial increase in the specific energy deposition (per single CO molecule) under decreasing CO concentration noticeably changes electron energy balance in the discharge. As the CO concentration falls, the part of a pump energy spent to excite electronically excited states increases, and the part of the power used for vibrational excitation of CO molecules in the discharge reduces. This effect is illustrated in Fig. 9 where the balances of electron power in the discharge are shown, which are calculated by solving stationary Boltzmann equation for the CO : He = 1 : 10 and 0.3 : 10 mixtures.

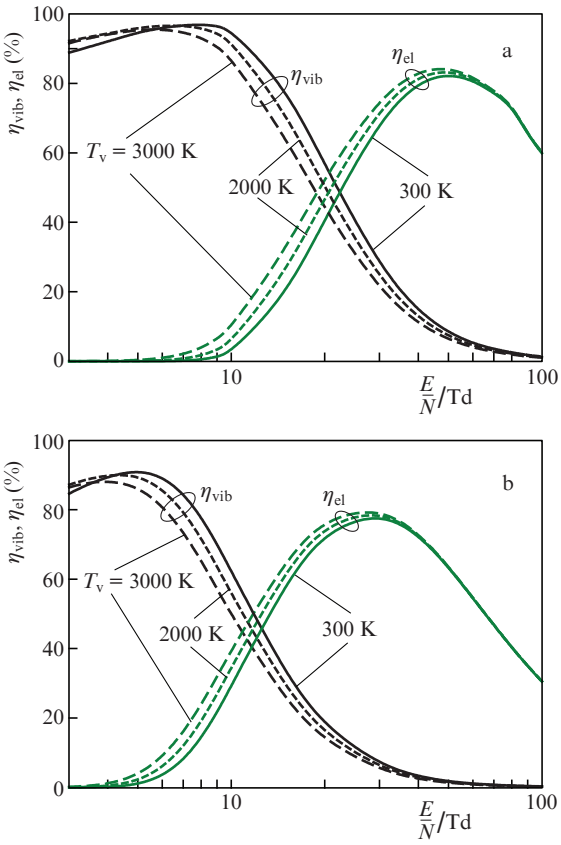

Figure 9. Calculated parts of a pump power deposited into a discharge, expended to excitation of molecule vibrations (η_{vib}) and electron-excited states (η_{el}) at various values of CO molecule vibrational temperatures T_v on the first vibrational level in the mixture CO : He = (a) 1 : 10 and (b) 0.3 : 10.

The results agree with experimental study [24] of long-term dynamics of luminescence spectra for the active medium of a slab cryogenic RF-discharge-pumped CO laser: during laser operation under stationary pumping conditions, starting from approximately the middle of the operation cycle, the intensity of luminescence of the CO molecule electronically excited states corresponding to the transition band $b^+\Sigma^+ \rightarrow a^1\Pi$ sharply increased. In addition, the calculation results presented in Fig. 9a agree with the approximation chosen for modelling the kinetics of the active medium (see Section 2).

Thus, additional calculations performed for various laser characteristics show a sufficiently good agreement between theory and experiment.

3.5. Contribution of plasma-chemical processes to changes in the active medium composition

The onset of lasing on overtone transitions of the CO molecule through a certain time interval after switching on the pulse-periodic RF-discharge points to a substantial reduction of molecular oxygen concentration in the active volume (in the space between electrodes) of a slab cryogenic CO laser at this moment, which is related to O_2 dissociation by plasma electrons. In this case, oxygen atoms participate in restoring the concentration of CO molecules [28], which increases the time of laser stable operation as compared to that in an oxygen-free gas mixture.

One more substantial factor for stable laser operation may be processes of ozone production ($O_2 + O + M \rightarrow O_3 + M$), which partially freezes on cold elements of a laser chamber and is present in a discharge gap and buffer volume in the form of vapours not affecting the vibrational kinetics of the CO laser active medium. In this case, ozone, participating in the heterogeneous chemical reactions, which result in CO molecule regeneration, decelerates degradation of the active medium. Possibly, one more channel for CO regeneration is the $C(^3P) + O_2(X^3\Sigma_g^-) \rightarrow CO(X^1\Sigma^+,v) + O(^3P)$ reaction, which leads to production of vibrationally excited CO molecules [28, 29]. A detailed consideration of plasma-chemical processes with participation of ozone and atomic carbon in the active medium of a cryogenic CO laser requires additional experimental study.

4. Conclusions

The influence of molecular oxygen addition to an active medium of a cryogenic overtone RF-discharge-pumped CO laser operated without forced active medium recirculation on the threshold conditions of arising laser generation is calculated. Calculation results of spectral and energy characteristics of laser radiation revealed their good agreement with the experimental data obtained immediately after switching on the discharge, and a substantial distinction from data obtained after reaching the steady-state operation regime. Calculation results concerning the temporal radiation pulse profiles of the CO laser operating on fundamental band transitions well agree with experimentally measured data. The substantial changes in characteristics of the laser as it reaches the stationary operation regime are related to relatively slow changes in the gas mixture composition as in the ballast volume so and in the discharge gap. These changes are explained by volume tric and heterogeneous plasma-chemical processes in the active medium of the laser.

Acknowledgements. The work was supported by the Russian Foundation for Basic Research (Project No. 18-02-00920).

References

1. Patel C.K.N. *Phys. Rev*., **141** (1), 71 (1966).
2. Ionin A.A., in: *Entsiklopediya nizkotemperaturnoi plazmy* (Encylcopedia of Low-Temperature Plasma). Ed. by S.I. Yakovlenko (Moscow: Fizmatlit, 2005) Ser. B, Vol. XI-4, p. 740.
3. Ionin A.A., in *Gas Lasers*. Ed. by M. Endo, R.F. Walter (Boca Raton: CRC Press, Taylor & Francis Group, 2007) p. 201.
4. Ionin A.A., Kurnosov A.K., Napartovich A.P., Seleznev L.V. *Laser Phys*., **20** (1), 144 (2010).
5. Bachem E., Dax A., Fink T., Weidenfeller A., Schneider M., Urban W. *Appl. Phys. B*, **57**, 185 (1993).
6. Averin A.P., Babaev I.K., Basov N.G., Ionin A.A., Petrakovskii V.V., Semenov S.V., Sinitsyn D.V., Uryasev A.V., Khar'kovskii P.N., Cheburkin N.V., Churbakov S.V., Yugov V.I. *Sov. J. Quantum Electron*., **20** (5), 493 (1990) [*Kvantovaya Elektron*., **17** (5), 561 (1990)].
7. Borodin A.M., Gurashvili V.A., Kuz'min V.N., Kurnosov A.K., Napartovich A.P.,Turkin N.G., Shchekotov E.Yu. *Quantum Electron*., **26** (4), 307 (1996) [*Kvantovaya Elektron*., **23** (4), 315 (1996)].
8. Jianguo X., Wang Z., Wentao J. *Appl. Phys. Lett*., **75**, 1369 (1999).
9. Kiselev V.V., Mineev A.P., Nefedov S.M., Pashinin P.P., Goncharov P.A., Drozdov A.P. *Lazernaya fizika i opticheskie tekhnologii: materialy IX mezhdunarodnoi nauchnoi konferentsii* (Laser Physics and Optical Technologies: Materials of IX International Scientific Conference) (Grodno: GrGU, 2012) p. 44.
10. Mineev A.P., Nefedov S.M., Pashinin P.P., Goncharov P.A., Kiselev V.V., Drozdov A.P. *Vestnik Vozdushno-Kosmicheskoi Oborony*, No. 3 (7), 47 (2015).
11. Ionin A.A., Kozlov A.Yu., Seleznev L.V., Sinitsyn D.V. *Quantum Electron*., **39** (3), 229 (2009) [*Kvantovaya Elektron*., **39** (3), 229 (2009)].
12. Ionin A.A., Kozlov A.Yu., Seleznev L.V., Sinitsyn D.V. *IEEE J. Quantum Electron*., **45** (3), 215 (2009).
13. Ionin A.A., Kozlov A.Yu., Seleznev L.V., Sinitsyn D.V. *Opt. Commun*., **282**, 629 (2009).
14. Ionin A.A., Kozlov A.Yu., Rulev O.A., Seleznev L.V., Sinitsyn D.V. *Appl. Phys. B: Las. Opt*., **122**, 183 (2016).
15. Mikheyev P.A., Ufimtsev N.I., Demyanov A.V., Kochetov I.V., Azyazov V.N., Napartovich A.P. *Plasma Sources Sci. Technol*., **19**, 025017 (2010).
16. Ionin A.A., Sinitsyn D.V., Terekhov Yu.V., et al. *Fiz. Plazmy*, **31**, 848 (2005).
17. Ionikh Yu.Z. *Opt. Spektrosk*., **51** (1), 76, (1981).
18. Billing G.D., Coletti C., Kurnosov A.K., Napartovich A.P. *J. Phys. B: At., Molec. Opt. Phys*., **36**, 1175 (2003).
19. Ionin A.A., Klimachev Yu.M., Kozlov A.Yu., Kotkov A.A., Kurnosov A.K. *Quantum Electron*., **38** (9), 838 (2008) [*Kvantovaya Elektron*., **38** (9), 838 (2008)].
20. Raizer Yu.P. *Gas Discharge Physics* (Berlin: Springer, 1991; Moscow: INTELLEKT, 2009).
21. Kikoin I.K. (Ed.) *Tablitsy fizicheskikh velichin. Spravochnik* (Tables of Physical Quantities: A Handbook) (Moscow: Atomizdat, 1976).
22. Grigoriev I.S., Meilikhov E.Z. (Eds) *Handbook of Physical Quantities* (Boca Raton, NY: CRC Press, 1996; Moscow: Energoatomisdat, 1991).
23. Wahid M.S., Madhusudana C.V. *Intern. J. Heat Mass Transfer*, **43**, 4483 (2000).
24. Ionin A.A., Kozlov A.Yu., Seleznev L.V., Sinitsyn D.V. *Fiz. Plazmy*, **43** (4), 267 (2017).
25. Maksimov A.I., Polak L.S., Sergienko A.F., Slovetskii D.I. *Khim. Vys. Energ*., **13** (4), 358 (1979).
26. Grigoryan G.M., Ionikh Yu.Z. *Khim. Vys. Energ*., **23** (4), 548 (1989).
27. Aleinikov V.S., Masychev V.I. *Lazery na okisi ugleroda* (Carbon Monoxide Lasers) (Moscow: Radio i Svyaz', 1990).
28. Trubachev E.A. *Trudy FIAN*, **102**, 3 (1977).
29. Jans E., Frederickson K., Yurkovich M., Musci B., Rich J.W., Adamovich I.V. *Chem. Phys. Lett*., **659**, 112 (2016).